NASA
Technical Memorandum 83490

AVRADCOM
Technical Report 83-C-11

Ceramic Composite Liner Material For Gas Turbine Combustors

Daniel B. Ercegovic and Curtis L. Walker
Propulsion Laboratory
AVRADCOM Research and Technology Laboratories
Lewis Research Center
Cleveland, Ohio

and

Carl T. Norgren
Lewis Research Center
Cleveland, Ohio

Prepared for the
Twenty-second Aerospace Sciences Meeting
sponsored by the American Institute of Aeronautics and Astronautics
Reno, Nevada, January 9-12, 1984

NASA

CERAMIC COMPOSITE LINER MATERIAL FOR GAS TURBINE COMBUSTORS

David B. Ercegovic and Curtis L. Walker

Propulsion Laboratory
AVRADCOM Research and Technology Laboratories
Lewis Research Center
Cleveland, Ohio

and

Carl T. Norgren

National Aeronautics and Space Administration
Lewis Research Center
Cleveland, Ohio

ABSTRACT

Advanced commercial and military gas turbine engines may operate at combustor outlet temperatures in excess of 1920K (3000°F). At these temperatures combustors liners experience extreme convective and radiative heat fluxes. The ability of a plasma sprayed ceramic coating to reduce liner metal temperature has been recognized. However, the brittleness of the ceramic layer and the difference in thermal expansion with the metal substrate has caused cracking, spalling and some separation of the ceramic coating. Research directed at turbine tip seals (or shrouds) has shown the advantage of applying the ceramic to a compliant metal pad. This paper discusses recent studies of applying ceramics to combustor liners in which yttria stabilized zirconia plasma sprayed on compliant metal substrates which were exposed to near stoichiometric combustion, presents performance and durability results, and describes a conceptual design for an advanced, small gas turbine combustor. Test specimens were convectively cooled or convective-transpiration cooled and were evaluated in a 10 cm square flame tube combustor at inlet air temperatures of 533K (500°F) and at a pressure of 0.5 MPa (75 psia). The ceramics were exposed to flame temperatures in excess of 2100 K (3320°F). Results appear very promising with all thirty specimens surviving a screening test and one of two specimens surviving a cyclic durability test.

INTRODUCTION

The current trend in advanced military and commercial transport engines is to fuel efficient, durable, and environmentally acceptable engines of ever increasing pressure ratio and turbine inlet temperature. This trend has produced a more severe environment in which the entire hot section, and in particular the combustor liner, must operate.

Ceramic materials offer distinct advantages in combustors by reducing the required quantity of air used for liner cooling. The practical limit for most metal liners is near 1100K and requires substantial quantities (near 50%) of the total combustor airflow for cooling. Ceramics can withstand bulk temperatures near 1650K and thus require significantly less air for cooling.

Small gas turbine combustors, and in particular, small reverse flow annular combustors, exhibit the highest cooled surface area to combustor volume ratio. These combustion systems therefore require some of the highest cooling air flows for their survival. As engine cycle temperatures approach 1920 K for these engines, it has become extremely difficult to design a satisfactory high temperature reverse flow annular combustor. The felt-ceramic concept, though by no means fully developed, offers the high temperature performance of a ceramic, plus the potential damage tolerance of a ductile metallic substrate. The introduction of these materials, if feasible, into this engine size may begin to open a new plateau of performance and efficiency.

The control and management of the air freed by the use of advanced technology liners has been a very successful approach to controlling emissions and improving combustor durability (refs. 1 & 2). Also, the hotter liner walls obtainable with ceramics will reduce the unburned hydrocarbon and carbon monoxide emissions that arise from liner thermal quenching of the combustor reactions during part power operation (ref. 3).It may now be possible to take advantage of these benefits of ceramics by the introduction of a compliant, low density sintered metal layer between a thick ceramic and a solid metallic substrate. This technique reduces the thermal stresses in the ceramic and allows the pressure stresses to be absorbed by the metallic substrate. This property may avoid ceramic spallation during thermal cycling of the liner.

Although relatively little work has been done to investigate the use of ceramic materials as combustor liners, significant research has been conducted in the application of ceramics to turbine gas path seal systems. Systems based on hot-pressed silicon carbide (SiC) and Si-SiC composites (ref. 4), ceramic honeycombs (ref. 5), sintered zirconium dioxide (ZrO_2) (ref. 6), and plasma sprayed ZrO_2 (ref. 7) have been

assessed for use as seal systems. Of these, the greatest activity is in perfecting systems utilizing plasma sprayed yttria stabilized ZrO_2 for resistance to cracking and spalling caused by thermally induced stresses; and oxidation caused by prolonged exposure to high temperatures. There are two methods known for reducing or minimizing the thermal stress generated in a plasma sprayed ZrO_2 seal system. These methods are shown in figure 1. One is to grade the material properties in a stepwise or continuous manner by grading the material composition from fully metallic adjacent to the substrate to fully ceramic adjacent to the gas path. This method is summarized in reference 7. The other method is to incorporate a low density, sintered metal pad or compliant layer between the ceramic layer and the metallic substrate, as described by Erickson (ref. 8). This strain isolator will elastically absorb the stresses generated during thermal cycling by the mismatch in the coefficients of thermal expansion of the ceramic and metal and by the difference in temperature of the ceramic and metal components. Applying a thin NiCrAlY bond coat developed by Stecura (ref. 9) to the system with the low modulus pad gave this system particularly good resistance to thermal shock failure (ref. 10). The work of Bill (ref. 11) compares both of these methods under similar test conditions. He concluded that the low modulus substrate approach proved to be more effective for reducing thermal stresses in the ceramic layer and preventing spalling than were the sprayed, graded composition approaches. To minimize the temperature at the interface between the ceramic layer and the low density sintered metal layer and therefore hopefully increase the specimens life, a transpiration cooled derivative of the low modulus substrate design was also investigated.

Sokolowski (ref. 12) has shown that the current trend in advanced combustor liner designs is to a segmented shingle approach. For this reason the low modulus substrate concept was configured into a test specimen of approximate size for a turbofan engine combustor liner segments as shown in figure 2.

This report will discuss combustor evaluations of thirty combustor liner specimens fabricated by plasma spraying yttria stabilized zirconia on compliant low modulus substrates. Specimens were evaluated for thermal performance and durability. A conceptual design for an advanced, small gas turbine combustor is presented along with a description of critical areas for future research.

MATERIALS

The strain isolation pad materials chosen were Hoskins Alloy 875 BRUNSBOND (R) pad, and BRUNSLLOY (R) 534 Fiber Metal pad. Hoskins 875 is a FeCrAl composition, and BRUNSLLOY (R) 534 is a FeNiCrAlY composition alloy. Two pad thicknesses, 0.25 and 0.38 cm, were investigated for each pad material. Also, two density levels, 35% and 45%, were investigated for each material.

The ceramic coatings chosen for investigation were calcium silicate ($CaSiO_2$) and two yttria stabilized zirconias, Metco 202 (19% Y_2O_3-ZrO_2) and Zircoa's 8% Y_2O_3-ZrO_2. Ceramic powders were plasma sprayed to thicknesses of 0.19 and 0.33 cm. The lower limit was determined by successful turbine shroud seal designs and the upper limit by the desire to investigate thick ceramics as set by the maximum limit capability of the plasma spray process used.

The backing for all specimens was a 0.08 cm thick Inconel Alloy 718 sheet. All backing sheets had sixteen 0.10 cm diameter holes Electric Discharge Machined (EDM) along the front and back edges to cool the attachment areas.

All felt pads were brazed to Inconel 718 backing plates after EDM completion using a high temperature nickel base braze compatible with both the felt and backing as described in reference 13. After brazing, the specimens were inspected and cleaned by alumina grit blasting immediately prior t application of a bond coat. All specimens were plasma sprayed with a 0.008 to 0.013 cm thick Ni-16.2 Cr-5.5 Al-0.6Y bond coat. Specimens were then plasma spray coated with the selected ceramic in a continuous spray to the desired thickness as tabulated in table 1. Transpiration cooled specimens were fabricated in the same manner as the convectively cooled specimens described above and are shown in figure 3. These specimens contained 3 arrays totaling 44 counter flow cooling passages 0.13 cm wide and 1.9 cm long and 0.13 cm deep.

APPARATUS AND PROCEDURE

The gas turbine combustor test rig used for this evaluation is shown in figure 4. The test rig was designed and fabricated by General Applied Science Laboratory (GASL) of Westbury, New York. The experimental evaluation of the thirty test specimens was also conducted at GASL and is described in greater detail in reference 14. The test rig was designed as a segment of a large annular combustor and produces a premixed propane-air flame stabilized by a perforated plate flameholder. The hot section is 10 cm x 10 cm with film cooled liners as the top and bottom sections and ceramic coated water cooled sidewalls.

The combustor section is shown schematically in figure 5. This figure illustrates the placement of the felt ceramic test panels and the variable flow film cooling slot upstream of the felt ceramic panels. This cooling slot was designed to admit from 0% to 2% of the total combustor airflow to film cool the test panels. The panels were mounted 7 cm downstream of the flameholder exit plane.

All test specimens were instrumented with from three to nine thermocouples. Thermocouples were placed on the backsurface of the Inco 718 sheet, at the felt-backing interface, and at the ceramic-felt interface. All thermocouples were installed after completion of the plasma spray process used for specimen fabrication. Interface thermocouples were closed ball couples inserted into a hole drilled to the desired

interface depth. Backsurface thermocouples were open ball type spot welded to the backing. figure 6 depicts the location of thermocouples whose temperature data is presented later in this report.

The transpiration cooled specimens were calibrated in an atmospheric stand to determine the flow characteristics of the coolant passages for various pressure drops. During these measurements conducted both before and after hot testing, the edge cooling holes located along the front and back of the backing were sealed.

The felt-ceramic specimens were tested at an inlet pressure of 0.5 MPa, an inlet air temperature of 533K, a primary zone equivalence ratio of 0.93 with a resultant adiabatic flame temperature of 2170K. The differential pressure drop across the panels was 0.0163 MPa or 3% of the inlet air pressure. The combustor reference velocity was 25 m/sec. All specimens were convectively cooled on their back surfaces by bypass air at 493 K with a velocity of 13.6 m/s. The specimens were film cooled by 1% of the total entrance airflow of 0.83 kg/sec. The variable cooling air slot was incorporated to thermal protect the specimens in the event it was needed. A complete listing of all test conditions is presented in Table 2. For the transpiration cooled panels, the primary zone equivalence ratio was established as 0.88 $\pm$ 0.02. All other conditions were the same as Table 2 values.

Combustion testing was divided into screening tests and endurance tests. In the screening tests the conditions of Table 2 were maintained for 3 minutes, followed by a shutdown. The shutdown procedure involved an abrupt fuel shut-off to provide the greatest possible thermal shock, followed by a gradual cessation of air flow. This sequence was repeated four times.

Endurance testing was similar to screening testing except that the test conditions of Table 2 were maintained for 2 minutes, followed by a shutdown. This shutdown also invoved an abrupt fuel shut-off followed by a gradual cessation of air flow. This sequence was repeated 30 times. This 30 cycle sequence was run as 5 multiples of 6 cycles. Each multiple of 6 cycles was run at 24 hour intervals. This down time was required to reheat the nonvitiating pebble bed preheater used for these tests.

RESULTS AND DISCUSSION

Screening Tests

The operating conditions for the screening tests, discussed earlier, are given in Table 2. After conduct of the screening test on all 30 specimens, none of the panels showed any visible evidence of deterioration or failure except for the discoloration of the ceramic and back surfaces. There were no mudflat cracks, felt-ceramics separations, or felt-backing separations on any of the panels. The ceramic surfaces of all the panels, after the screening tests, are shown in figure 7. The black-grey material on the ceramic surfaces of panels #7 and #10 is a slag deposition from a flameholder burnout which occurred during an aborted screening test of these panels. The combustor rig was then repaired and these panels retested. They also displayed no visible signs of distress after testing.

It was expected that some of the specimens would have displayed varying degrees of distress after conduct of the screening tests, and that their physical condition would be the basis for their performance ranking. However, all post test inspections showed the specimens in excellent condition with no visible performance discriminators between them. Therefore, a combination of theory and experiment was employed to rank the performance of the various panel designs.

There are two areas critical to the performance of this low modulus substrate concept. First, the temperature at the felt-ceramic interface must be below approximately 1240 K to reduce or eliminate the growth of NiO oxidation nodules at this interface. The growth of these nodules results in oxidation induced cracks with subsequent ceramic spallation. Secondly, the ceramic layer itself must operate in a range where structurally and thermally induced stresses are not beyond the ceramic's capability.

Figure 8 depicts the measured thermocouple data for all 22 convectively cooled test specimens. The solid curves are theoretical heat transfer calculations based on ceramic and felt material properties published in references 10, 13, and 15. The thermal analysis was based on reference 16 for the overall characterization of the radiative and convective heat fluxes and on references 17 and 18 for the effects of the film cooling slot on the hot side convective heat flux.

The data of figure 8 displays extreme scatter in both the backing felt and felt-ceramic interface temperature data. Most measured interface temperatures appear well below the theoretical level. Although this scatter could be generated by non-uniform crosstream temperature and velocity profiles it is most likely caused by the partial failure of the majority of interface thermocouples. Previous attempts to measure the interface temperatures was done by welding thermocouples to the felt during the manufacturing process prior to plasma spraying the bond coat and the ceramic. Although this method provided accurate placement and measurement of the temperature, cyclic testing of these specimens resulted in failures at the thermocouple locations. For this reason closed ball thermocouples were installed after complete specimen fabrication. The thermocouple ball was held against the interface by the spring pressure of a NiCrAlY ribbon spot welded to the back of the specimen. It is felt that during thermal cycling of the specimen, this pressure was relaxed or removed resulting in loss of contact between the thermocouple and the interface. This phenomena would result in low measured temperatures. For this reason, a qualitiative theoretical method was used for the selection of the two specimens for durability testing.

Referring to figure 5 one can see that the axial edges of a the ceramic layer are constrained by a compressible fiberfax layer against the combustor side walls. Consequently, spanwise thermal expansion of the ceramic will produce only low compressive stresses. Since the compressive strength of the ceramic is high, these stresses are not likely to cause ceramic failure. The front and back edges of the ceramic, on the other hand, are free to move.

The temperature of the felt-ceramic interface governs the potential relative thermal expansion between the felt pad and ceramic layer, the strength of both materials, the thermally induced surface stress on the ceramic, and the oxidation resistance of the felt. At the measured values of the felt-ceramic interface temperatures, typically about 900K, the felt pad has a very low yield strength of about 7×10^6 N/m^2. Consequently, it is unlikely that the felt pad could produce a significant level of stress on the ceramic.

Full analysis of thermal stress induced failure of the ceramic panels requires detailed consideration of shutdown transient as well as steady state temperature distributions, interfacial shear stresses and normal stresses, and some ability to track changes in ceramic layer compliance as "mudflat" cracks develop. Such analysis requires accurate and detailed temperature distribution data, both transient and steady state, temperature dependent material properties, as well as cycle-to-cycle changes in ceramic compliance. It is recognized that failure mechanisms are driven by tensile stresses in the ceramic-bondcoat interface, and the time dependent effects of oxidation and stress relaxation driven by the temperature at the metal-ceramics interface and in the ceramic itself. Therefore given sufficient materials properties and the temperature distribution data, it is possible to calculate a critical stress. However given that the ceramic surface temperature must be implied from numerical calculations and all experimental interface temperature have high scatter, it was decided to merely rank the panels by their calculated temperature difference across the ceramic, which is proportional to the ma imum stress.

Table 3 presents the analytical temperature difference across the ceramic layer and the felt-ceramic interface temperatures for the specimen matrix of Table 1 at the mid-axis, mid-plane thermocouple locations of figure 6. This table assumes that the thermal properties of the two ceramics and the two felts tested are similar and that the thermal conductivity of the felt was dependent upon density.

This tabulation shows that increasing the ceramic thickness from 0.19 cm to 0.33 cm or 74% results in a 60% increase in the ceramic thermal gradient (ΔT) while only reducing the felt-ceramic interface temperature by approximately 3%. For 0.19 cm thick ceramic layers, increasing pad density from 35% to 45% dense increases ceramic ΔT's by 10% to 15% while decreasing felt-ceramic interface temperatures by approximately 5%. The lowest ceramic ΔT's occurred for the 0.19 cm thick ceramic coupled with the 35% density pad. In this combination of materials increasing pad thickness from 0.25 cm to 0.38 cm resulted in a 9% ceramic ΔT decrease but increased the felt-ceramic interface temperature by 4% and resulted in the highest felt-ceramic interface temperature of the entire matrix. For these reasons two specimens #7 and #28 were selected from the group of 0.19 cm thick ceramic, 0.25 cm thick 35% density felts for durability testing. These two specimens were both plasma sprayed with the 19% Y_2O_3 - ZrO_2 ceramic, with #7 fabricated of H875 pad material and #28 of H534 material.

Endurance Tests

After completion of the screening tests, panels #7 and #28 were selected from among the group exhibiting lowest stress level for further testing to evaluate their endura e characteristics. The selection criteria were low stress levels in panels with approximately the same properties but with different pad materials. These two specimens both had a 1.9 cm thick 19% Y_2O_3 - ZrO_2 ceramic over an approximately 35% dense 2.5 cm thick pad. For exact specifications refer to Table 1.

These two specimens were then exposed to 30 thermal cycles to the conditions of Table 2 as previously described. Both panels completed the endurance test procedure without structural failure. Panel #7, shown in figure 10, shows some discoloration of the ceramic and back surface. A closeup view of the ceramic surface reveals mudflat cracks. These cracks are found over the surface and show no preferential location. The ceramic did not separate from the intermediate felt pad and there is no visible damage to the felt pad, the backing, or the felt-backing interface. The black-grey material seen on the ceramic surface of figure 10 is the slag deposition from the flameholder burnout noted earlier. Figure 11 depicts specimen #28 after the endurance test. This panel did display failure where 5 major cracks linked up over approximately 50% of the ceramic surface. Figure 12 depicts this same specimen after removal of the loose ceramic. The spalling that did occur was not limited entirely to the felt-ceramic interface as approximately 10% of the interface area in the spalling region is still covered with ceramic. Despite the fact that 50% of the ceramic surface was not attached to the pad, when the rig was disassembled after completion of the endurance tests, this loose ceramic was found inplace on the pad surface. The major loose pieces fell off as the specimen was removed from the rig and the missing piece in the center of figure 11 was damaged at this time. This failure would be indicative of critical internal ceramic stresses. The complete survival of specimen #7 may indicate the superiority of the H875 pad material when compared to specimen #28 which is otherwise similar except that the pad is of H 534 alloy. However, the success or failure of the single test does not present a satisfactory statistical basis for firm conclusions about the superiority of H875 pad material at this time.

Transpiration Cooled Specimen Tests

The flow characteristics of the eight transpiration cooled panels, identified in Table 1, were measured in an atmosphereic discharge test stand both before and after undergoing screening tests. The mass flow results are shown in figure 9. The various panels were all designed to yield the same mass flow rate for a given pressure drop. This design goal is essentially verified by the results and, as expected, the measured mass flow rate is proportional to the square root of the pressure drop. An average 12% decrease in the mass flow rate of all panels is observed after undergoing combustion testing. This is due to oxidation of the felt pad material which tends to reduce its porosity. This trend may have a significant effect upon the service life of the specimens if oxidation closure of the coolant passages continues at this rate.

The backsurface temperatures recorded for the transpiration cooled specimens are tabulated in Table 4. Using the pre-test flow calibrations of figure 9, each transpiration cooled specimen flowed 0.015 kg/s or approximately 2% of the total combustor airflow. The temperatures recorded are remarkably cool and certainly attest to the efficiency of transpiration cooling.

Since there were no interface thermocouples installed in the transpiration cooled specimens, and the analytical heat transfer model used to predict interface and ceramic surface temperatures of the convective cooled specimens could not model the transpiration cooling, no calculations were performed on these specimens. It is expected that the transpiration cooling would have a similar effect of reducing the felt-ceramic and ceramic surface temperatures.

If the transpiration cooling scheme were to be applied to a typical axial, annular modern small gas turbine combustor, it would require approximately 12% of the total combustor airflow for liner cooling. This compares most favorably with the current requirement of approximately 50% of the total combustor airflow for liner cooling.

SUMMARY OF RESULTS

Experiments were conducted to evaluate a new felt-ceramic composite material for use as a combustor liner material. Experiments included a combustor screening test of 22 convectively cooled and 8 transpiration cooled specimens and a 30 cycle endurance test of 2 specimens to near stoichiometric combustion temperatures.

Combustor screening tests exposed all 30 test specimens to temperatures of 2170 K for 4 cycles. These tests did not experimentally discriminate between the test specimens as all 30 specimens showed no visible evidence of deterioration or failure except for discoloration of the ceramic and back surfaces. There were no mudflat cracks, felt-ceramic or backing-felt separations on any of the panels. The transpiration cooled specimens clearly documented the ability of this cooling scheme to keep the backsurface temperature and therefore all interface and ceramic surface temperatures extremely cool. While the convectively cooled specimens recorded backsurface temperatures near 900 K, the transpiration cooled specimens were typically less than 550 K. A combination of experimental data, theoretical heat transfer calculations, and fundamental stress analyses was therefore used to select 2 specimens for the durability tests.

Combustor durability tests exposed 2 selected test specimen configurations thought to have the lowest internal ceramic stresses based on low indicated temperature gradients, to temperatures of 2170 K for 30 thermal cycles. This repeated thermal cycling produced non-linking, non-catastrophic mudflat cracks in the ceramic coating of one test specimen and caused partial ceramic separation from the felt pad in the other test specimen.

The results of this program suggest the superiority of a system composed of the BRUNSBOND (R) H-875 compliant pad at approximately 0.25 cm thickness and 35% density, coupled with a NiCrAlY bond coat and a 8% Y_2O_3 - Z_rO_2 ceramic top coat of approximately 0.19 cm thickness. Results also indicate the outstanding cooling performance of the transpiration cooling scheme and the need to further investigate this system.

FUTURE APPLICATIONS

The benefit of a felt-ceramic composite liner in a gas turbine combustor is primarily realized by operating the engine at elevated temperatures which results in improved engine cycle efficiency. However, many problems currently exist and must be resolved before a viable felt-ceramic combustor concept can be demonstrated. Composite matrix properties such as ceramic type and thickness, pad type, thickness and density, and substrate selection must be determined. These properties should be optimized by a unified design system taking into account the fundamental characteristics of the individual materials and the required aerothermal performance of the combustor. Although numerous difficulties currently exist, the technology to solve these problems is within the realm of feasibility. In particular, the composite matrix properties need to be integrated into a 3-D finite element structural analysis.

Preliminary evaluation reported herein has shown that the integrity of the ceramic can be maintained even when exposed to near stoichiometric combustion temperatures with backside cooling provided by convection or by pseudo-transpiration techniques. A proposed design for a combustor applicable to a small gas turbine engine is shown in figure 13. This design takes advantage of a simple circumferentially stacked ring construction which minimizes axial stresses. In this design the thickness and density of the ceramic layer and the substrate can be varied from zone to zone to account for the differences in cooling requirements imposed by the combustion gases and the backside coolant

flows in each zone. The stacked ring construction also has the potential for lower manufacturing cost, the elimination of the sealing problems inherent with segmented tile construction, simpler mounting to the engine casing, and elimination of flame tube annulus blockage present in a segmented tile design.

While the composite liner approach is potentially applicable to most high temperature combustors where high cycle efficiency and low specific fuel consumption is paramount, the example selected is related to small advanced gas turbine engines. Due to the inherent geometric constraints a small combustor has a relatively large surface-to-volume ratio as compared to large combustors. If in addition a reverse-flow design is considered the surface-to-volume ratio is even more critical. Thus, due to the large cooling requirements the greatest potential and hence, the greatest benefit exist for composite application in the small combustor.

While a reverse-flow design is presented in figure 13, the principle is equally applicable to axial configurations. It would be expected that performance improvements would be most dramatically achieved in the smaller combustor because of the narrow annular height and the influence of wall quenching on part power efficiency and pollutant generation, whereas, in the larger systems wall effects would be expected to be less pronounced.

ACKNOWLEDGEMENTS

The authors would like to thank Mr. Jack Brown of NASA for plasma spray fabrication of the test specimens and Mr. R. S. Venkat Raman and Dr. Gerald Roffe for the conduct of the evaluation program at General Applied Science Laboratory.

REFERENCES

1. Greene, W., Tanrikut, S., and Sokolowski, D. E., "Development and Operating Characteristics of an Advanced Two-Stage Combustor," AIAA Paper 82-0191, Jan. 1982.

2. Tanrikut, S., Marshall, R. L., and Sokolowski, D. E., "Improved Combustor Durability-Segmented Approach with Advanced Cooling Techniques," AIAA Paper 81-1354, July 1981.

3. Dodds, W. J., Gleason, C. C., and Bahr, D. W., "Aircraft Gas Turbine Low-Power Emissions Reduction Technology Program - Final Report," General Electric Co., Cincinnati, Oh., R78AEG408, Oct. 1978. (NASA CR-135434)

4. Schwab, R. C. and Darolia, R., "Feasibility of SiC Composite Structures for 1370° C Gas Turbine Seal Applications," General Electric Co., R77AEG160-10, 1977.

5. Solomon, N. G. and Vogan, J. W., "Advanced Ceramic Material for High Temperature Turbine Tip Seals," International Harvester Co., San Diego, CA., RDR-1831-23, Jan. 1978. (NASA CR-135319)

6. Schlike, P. W., "Advanced Ceramic Seal Program - Phase I," Pratt & Whitney Aircraft, PWA 6635, Apr. 1974. (AD-781004)

7. Bill, R. C., Shiembob, L. T., and Stewart, O. L., "Development of Sprayed Ceramic Seal System for Turbine Gas Path Sealing," NASA TM-79022, 1978.

8. Erickson, A. F., Nablo, J. C., and Panzera, C., "Bonding Ceramic Materials to Metallic Substrates for High-Temperature low Weight Applications," ASME Paper 78-WA/GT-16, Dec. 1978.

9. Stecura, S., "Two-Layer Thermal Barrier Coating for High Temperature Components," American Ceramic Society Bulletin, Vol. 56, No. 12, Dec. 1977, pp. 1082-1085.

10. Bill, R. C., and Wisander, D. W., "Preliminary Study of Cyclic Thermal Shock Resistance of Plasma-Sprayed Zirconium Oxide Turbine Outer Air Seal Shrouds," NASA TM-73852, 1977.

11. Bill, R. C., Wisander, D. W., and Brewe, D. E., "Preliminary Study of Methods for Providing Thermal Shock Resistance to Plasma-Sprayed Ceramic Gas-Path Seals," NASA TP-1561, May 1980.

12. Sokolowski, D. E. and Rohde, J. E., "The E^3 Combustors: Status and Challenges Energy Efficient Turbofan Engines," NASA TM-82684, 1981.

13. Tolokan, R. P., Nablo, J. C., and Brady, J. B., "Ceramic to Metal Attachment Using Low Modulus BRUNSBOND Pad," ASME Paper 81-GT-160, Mar. 1981.

14. Venkat, R. S. and Roffe, G., "Testing of Felt-Ceramic Materials for Combustor Application," General Applied Science Labs. Inc., Westbury, N.Y., 1983. (NASA CR-168103)

15. Liebert, C. H., "Emittance and Absorptance of the National Aeroanutics and Space Administration Ceramic Thermal Barrier Coating for Gas Turbine Engine Components," Thin Solid Films, Vol. 53, 1978, pp. 235-240.

16. Northern Research and Engineering Corporation, "The Design and Performance Analysis of Gas-Turbine Combustion Chambers," Vol. 1, NREC Report No. 1082-1, 1964.

17. Juhasz, A. J. and Marek, C. J., "Combustor Liner Film Cooling in the Presence of High Free-Stream Turbulence," NASA TN D-6360, 1971.

18. Tacina, R. R. and Marek, C. J., "Film Cooling in a Combustor Operating at Fuel-Rich Exit Conditions," NASA TN D-7513, 1974.

TABLE 1. – MATERIAL SPECIFICATION MATRIX FOR SPECIMENS EVALUATED IN SCREENING AND DURABILITY TESTS (ENTRIES INDICATE SPECIMEN SERIAL NUMBERS)

		H 875 Pad material				H 534 Pad material			
		35 percent density		45 percent density		32 percent density		42 percent density	
	Thickness	0.25 cm	0.38 cm	0.25 cm	0.38 cm	0.25 cm	0.38 cm	0.25 cm	0.38 cm
19 percent Y_2O_3-ZrO_2 Ceramic	0.19 cm	7 2T[a] 3T 4T	4	11	11	28 8T 9T 10T	21	33	19
	0.33 cm	8	5	12	18	29	22	35	20
8 percent Y_2O_3-ZrO_2 Ceramic	0.19 cm	10 5T		14	42	30 11T		36	23

[a]T indicates transpiration cooled specimens.

TABLE 2. - COMBUSTOR OPERATING CONDITIONS FOR SCREENING AND DURABILITY TESTS

Inlet air temperature, K	533±12
Inlet air pressure, MPa	0.50±0.02
Total airflow rate, kg/s	0.83±0.02
Primary zone airflow rate, kg/s	0.40
Overall combustor pressure drop, MPa	0.0306±0.002
Reference velocity, m/s	25
Total bypass duct flow, kg/s	0.215 (each duct)
Specimen backsurface coolant air temperature, K	493±12
Specimen mean backsurface coolant velocity, m/s	13.6
Differential pressure across specimen, MPa	0.0163±0.002
Primary zone equivalence ratio:	
Convectively cooled specimens	0.93±0.015
Transpiration cooled specimens	0.88±0.02
Adiabatic flame temperature:	
Convectively cooled specimens, K	2170±35
Transpiration cooled specimens, K	2082±33

TABLE 3. - ANALYTICAL TEMPERATURE ΔT ACROSS THE CERAMIC LAYER AND FELT CERAMIC INTERFACE TEMPERATURES FOR THE SPECIMEN MATRIX OF TABLE 1[a]

		Felt Pad				
		35 percent density		45 percent density		
	Thickness	0.25 cm	0.38 cm	0.25 cm	0.38 cm	
Ceramic	0.19 cm	109K	100K	120K	115K	Ceramic ΔT
		1059K	1100K	1004K	1028K	Felt-ceramic interface temp
	0.33 cm	173K	160K	189K	182K	Ceramic ΔT
		1025K	1065K	972K	994K	Felt-ceramic interface temp

[a]19 percent Y_2O_3-ZrO_2 and 8 percent Y_2O_3-ZrO_2 assumed to have the same thermal conductivity; and H875 and H534 pad materials assumed to have the same thermal conductivity.

TABLE 4. - BACKSURFACE TEMPERATURE MEASUREMENTS FOR TRANSPIRATION COOLED SPECIMENS DURING SCREENING TESTS

Specimen serial number	Backsurface temperature, K		
	Left[a]	Center[a]	Right[a]
2T[b]	552	552	542
3T	532	538	526
4T	541	555	531
5T	549	553	536
8T	530	532	540
9T	516	512	519
10T	520	525	529
11T	529	524	536

[a]Locations as per figure 6.
[b]T indicates transpiration cooled specimens.

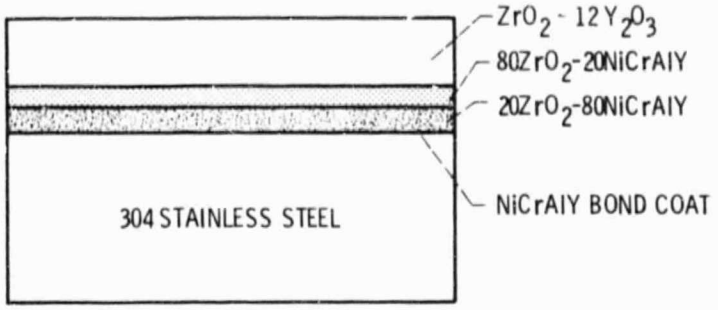

(a) Plasma-sprayed metal-ceramic intermediate layer concept.

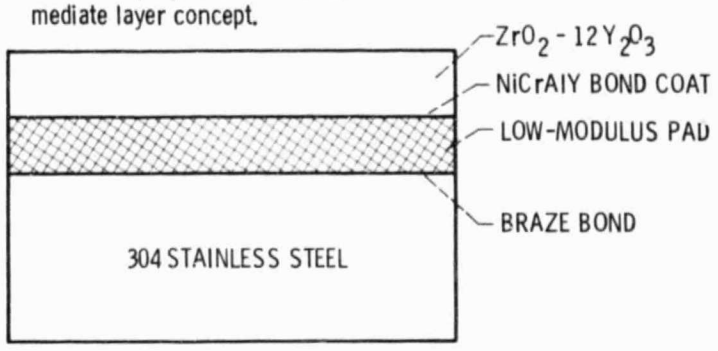

(b) Sintered-metal, low-modulus intermediate pad concept.

Figure 1. - Schematic representation of the two turbine seal concepts considered for use as a combustor liner material. (Compositions are in weight percent, (ref. 11).)

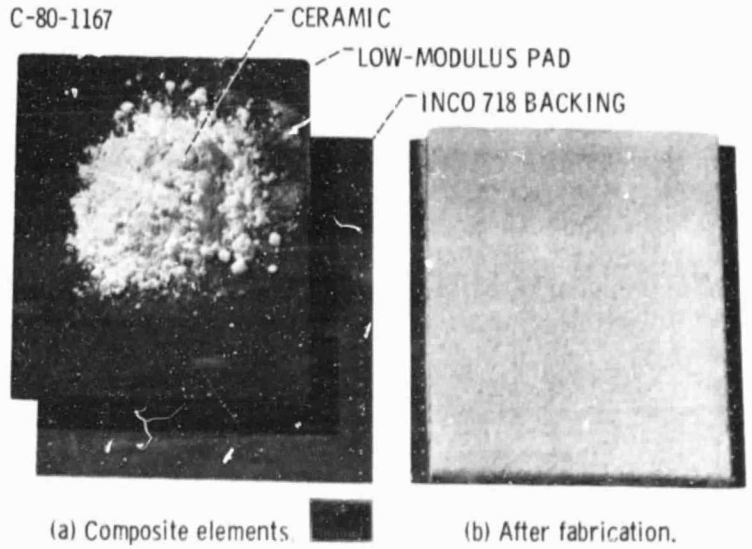

(a) Composite elements. (b) After fabrication.

Figure 2. - Felt-ceramic test specimens.

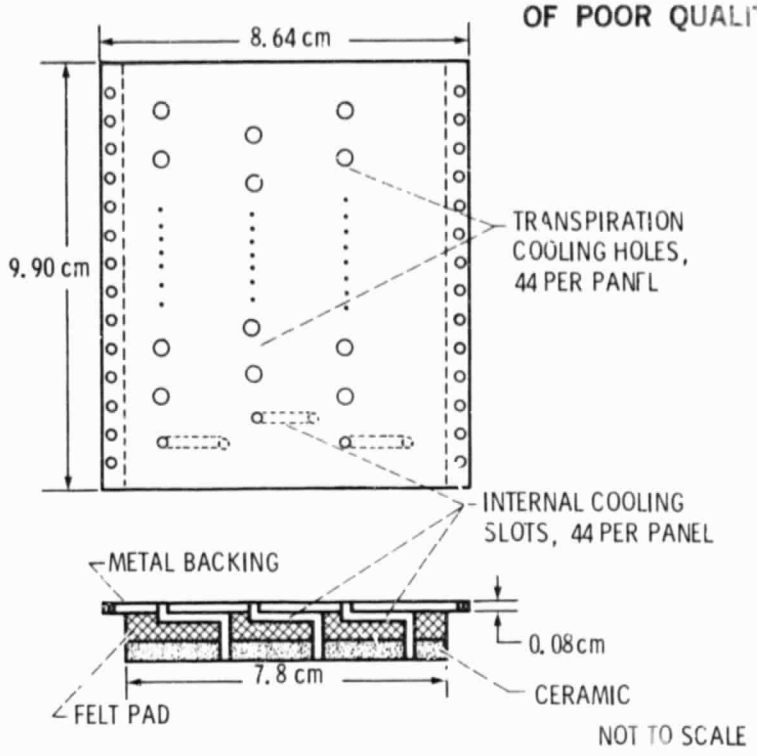

Figure 3. - Schematic of transpiration cooled felt-ceramic specimens.

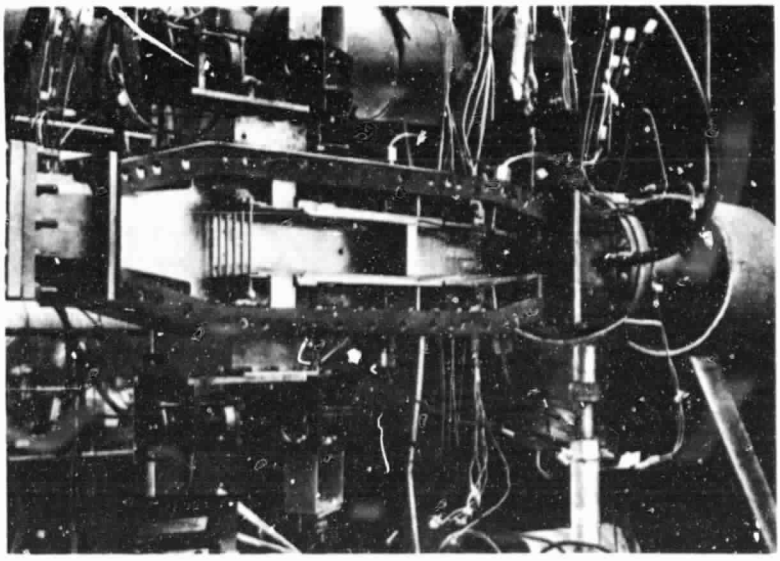

Figure 4. - Combustor rig used for screening and durability tests.

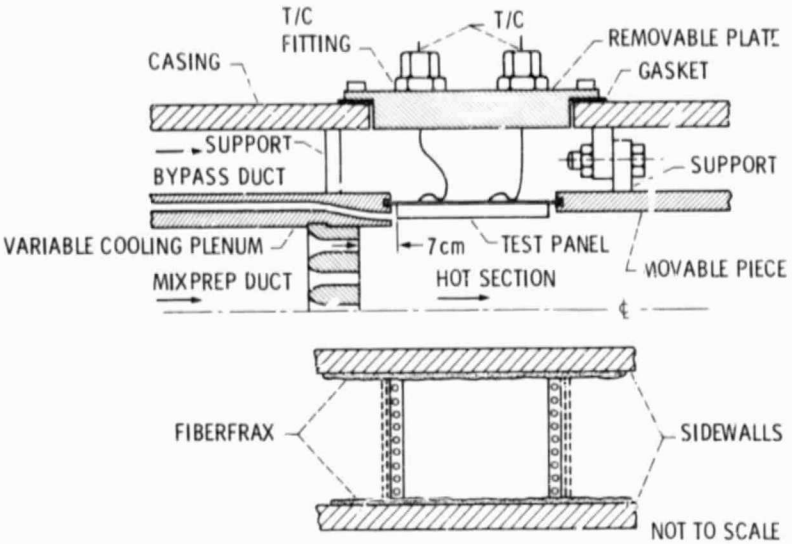

Figure 5. - Test panel installation details.

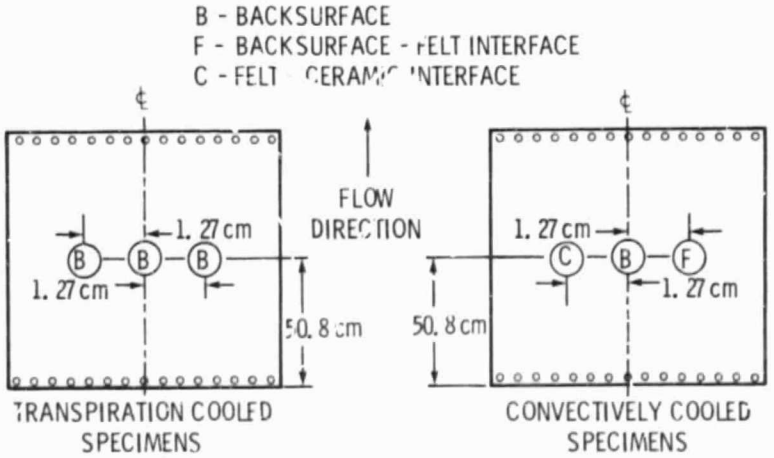

Figure 6. - Thermocouple installation locations.

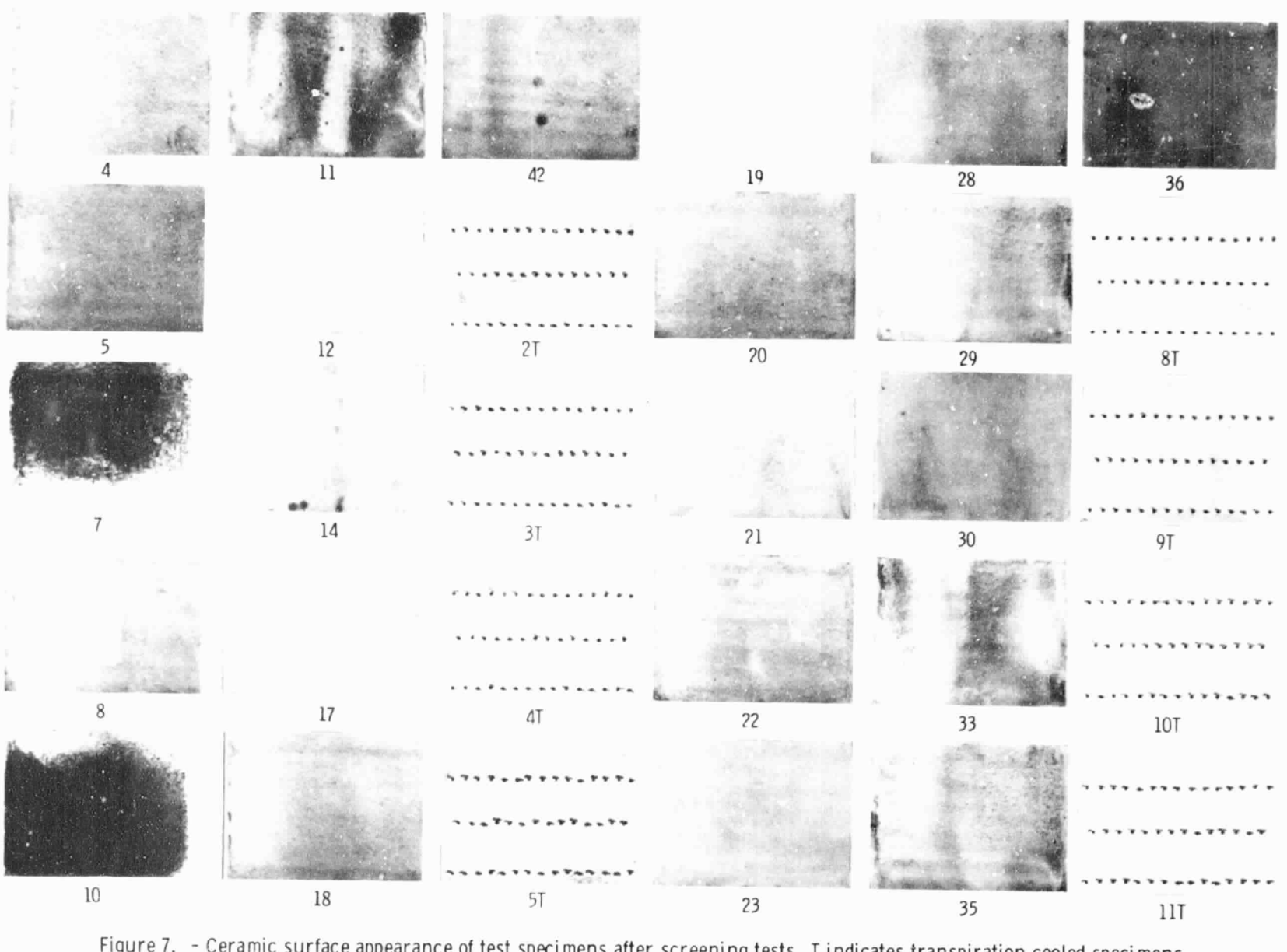

Figure 7. - Ceramic surface appearance of test specimens after screening tests. T indicates transpiration cooled specimens.

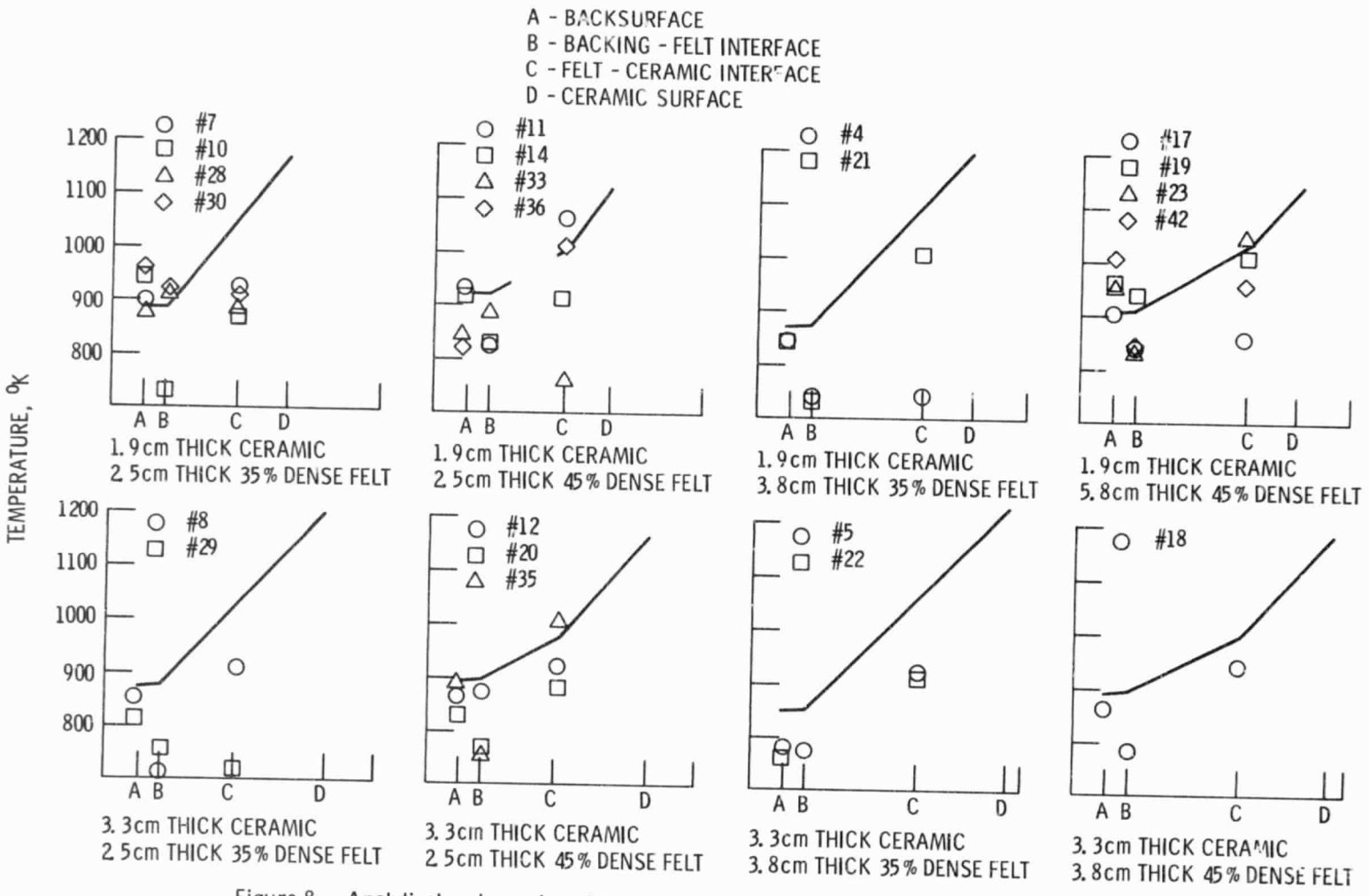

Figure 8. - Analytical and experimental test specimen temperatures measured during screening tests.

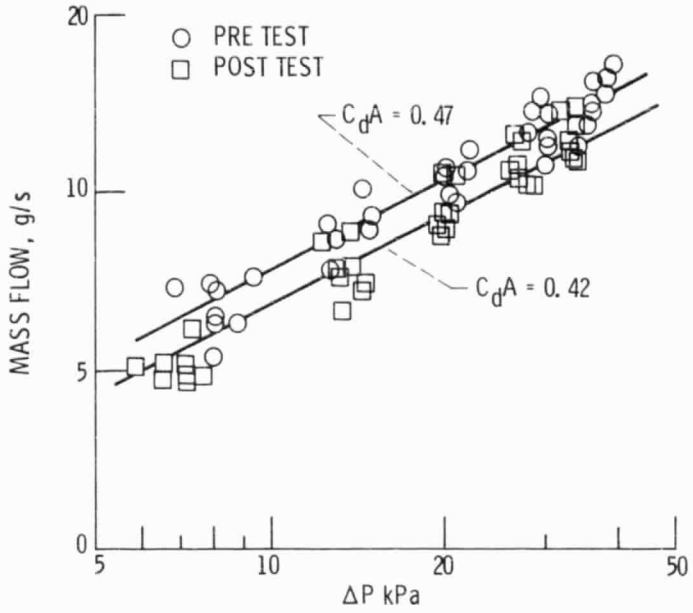

Figure 9. - Effect of screening test on flow characteristics of transpiration cooled specimens.

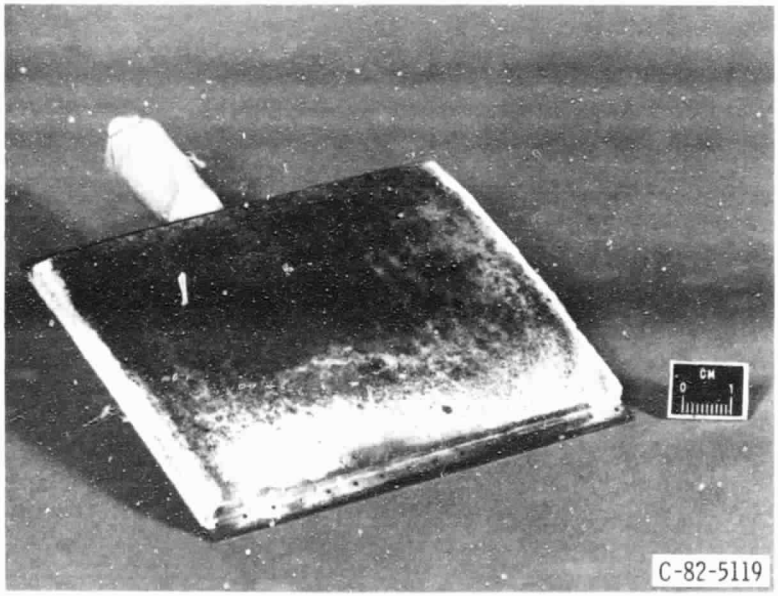

Figure 10. - Ceramic surface appearance of specimen #7 after durability tests.

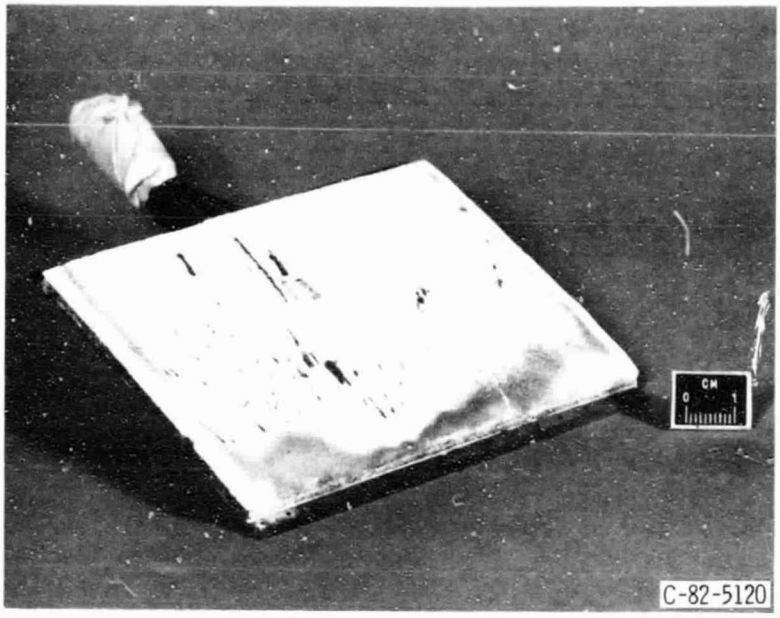

Figure 11. - Ceramic surface appearance of specimen #28 after durability tests.

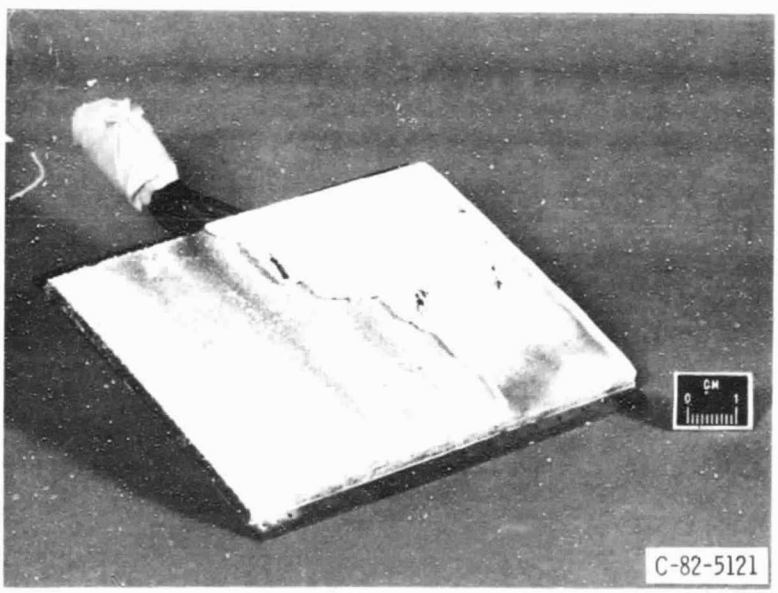

Figure 12. - Ceramic surface appearance of specimen #28 after durability test and removal of loose ceramic coating.

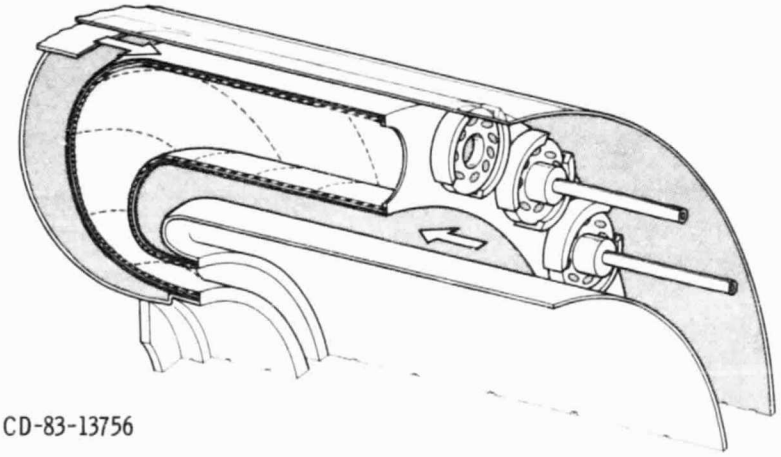

CD-83-13756

Figure 13. - Felt-ceramic combustor concept for advanced small reverse flow combustor.